

Power-exponential velocity distributions in disordered porous media

Maciej Matyka,* Jarosław Gołębiewski, and Zbigniew Koza

Faculty of Physics and Astronomy, University of Wrocław, 50-204 Wrocław, Poland

(Received 21 September 2015; revised manuscript received 27 November 2015; published 11 January 2016)

Velocity distribution functions link the micro- and macro-level theories of fluid flow through porous media. Here we study them for the fluid absolute velocity and its longitudinal and lateral components relative to the macroscopic flow direction in a model of a random porous medium. We claim that all distributions follow the power-exponential law controlled by an exponent γ and a shift parameter u_0 and examine how these parameters depend on the porosity. We find that γ has a universal value $1/2$ at the percolation threshold and grows with the porosity, but never exceeds 2.

DOI: [10.1103/PhysRevE.93.013110](https://doi.org/10.1103/PhysRevE.93.013110)

I. INTRODUCTION

The physics of viscous flows through porous media is important in such diverse areas of technology as oil recovery, energy storage, and tumor treatment [1–3]. Such flows, however, are notorious for their complexity stemming both from randomness of the medium and complicated interactions of different fluid particles. Macroscopic parameters characterizing fluid transport in porous media, like permeability (the ability of a porous system to transmit fluids) depend on a multitude of geometry-related parameters such as porosity, granule or fracture shape and size distribution, and specific surface area. This dependency, however, is nonuniversal and to a large extent known only through phenomenology or approximate theories.

The complete information about the flow of an incompressible fluid in a particular porous sample is contained in the velocity field. While this quantity can be studied both experimentally [4–8] and numerically [9,10], it is sample-dependent. Therefore, to get a better insight into the connection between the macroscopic properties of the flow and the irregular structure of the medium, one needs mathematical tools that take into account randomness of the porous matrix and filter out irrelevant, sample-dependent information contained in the full-velocity field. One such tool is the velocity distribution function (vdf) [4–6], which is the probability density function of the fluid velocity magnitude u or its longitudinal (u_L) or transverse (u_T) components. We will use a convenience notation f , f_L , and f_T to denote the vdfs corresponding to u , u_L , and u_T , respectively, and f_L^+ and f_L^- to denote f_L restricted to $\mathbb{R}_{>0}$ and $\mathbb{R}_{<0}$, respectively.

Unlike the famous Maxwell-Boltzmann distribution for the ideal gas, vdfs for a fluid flow reflect the structure of the medium rather than the effect of the interparticle collisions. Despite this difference, the vdfs are also closely related to important macroscopic parameters. For example, f and f_L immediately imply the value of the hydraulic tortuosity (τ) [11], a quantity that measures the mean elongation of fluid paths in a porous medium,

$$\tau \equiv \frac{\langle u \rangle}{\langle u_L \rangle} = \frac{\int_V f(u)u \, du}{\int_V f_L(u_L)u_L \, du_L}, \quad (1)$$

where the integrals are taken over the volume V of the porous sample. Similarly, for flows obeying Darcy's law [12], e.g., groundwater flows, the permeability (κ) can be related to the mean fluid velocity along the macroscopic flow direction,

$$\kappa = \varphi \mu \frac{\langle u_L \rangle}{|\nabla P|}, \quad (2)$$

where φ is the porosity of the medium (the ratio of the volume of voids to the total volume), μ is the dynamic viscosity of the fluid, and ∇P is the pressure gradient. Thus, the vdfs can serve as a link between two macroscopic parameters, κ and τ .

Several reports on f , f_L , and f_T for various porous systems at low Reynolds number ($\text{Re} \ll 1$) are already available. Physically, for arguments much smaller than $\langle u \rangle$ their form is dominated by contributions from stagnant zones (dead-end pores and the volumes in the proximity of the fluid-solid boundary) [9], whereas for arguments $\gtrsim \langle u \rangle$ their form reflects the properties of the conducting backbone, or the fluid paths carrying most of the fluid transport. For this reason the vdf is usually investigated in two physically distinct regimes: small ($u \lesssim \langle u \rangle$) and high ($u \gtrsim \langle u \rangle$) fluid velocities. In the former case, the local fluid kinetic energy at percolation follows a power law [9], which implies a similar, power-law behavior for $f(u)$, $u \ll \langle u \rangle$. Far from percolation, however, the form of $f(u)$ for small u depends on the porous matrix structure [13] and appears to be nonuniversal, therefore it will not be considered here.

In contrast to the case of small velocities, the available results suggest the existence of some universality in the form of the vdfs for $u \gtrsim \langle u \rangle$. The findings of different research groups, however, appear to be inconsistent with each other. On the one hand, several theoretical [5], experimental [5], and numerical [13,14] results suggest that $f(u)$ can be approximated by a Gaussian with the maximum shifted toward the mean fluid velocity. On the other hand, however, several teams reported nearly exponential vdfs with the maximum located at 0. This includes an experimental study on f , f_L^+ , and f_T [6], as well as experiments [4,15] and numerical simulations [15,16] for f_L^+ . Moreover, a qualitative transition from an exponential to a Gaussian form of f was found for various sphere packings [17]; however, in each case f peaked at $u = 0$. Finally, Siena *et al.* [18] suggested that f_L^+ follows the stretched exponential

*maciej.matyka@ift.uni.wroc.pl

function

$$f_L^+(u_L/\langle u_L \rangle) \propto (u_L/\langle u_L \rangle)^{\gamma-1} \exp[-\beta(u_L/\langle u_L \rangle)^\gamma], \quad (3)$$

where β, γ are model parameters.

Although Eq. (3) encompasses both the exponential and Gaussian distributions, it is not applicable to the systems with the distribution maximum shifted from 0. As a consequence, it predicts that the values of γ can be much larger than 2 [18], a result not corroborated by any other research.

To reconcile this difficulty, we conjecture that for $u \gtrsim \langle u \rangle$ the velocity distribution functions follow the power-exponential distribution,

$$f(u) = a \exp \left[- \left(\frac{u - u_0}{u_s} \right)^\gamma \right] \quad (4)$$

(and similar formulas for f_L^+ , f_L^- , and f_T), where $a > 0$ is the normalizing factor, $u_0 \geq 0$ determines the location of the distribution peak, $u_s > 0$ denotes the scale factor, and $0 < \gamma \leq 2$ is the shape factor. This is the simplest distribution that generalizes both the normal ($\gamma = 2$) and exponential ($\gamma = 1$) distributions and allows for the shift of the distribution maximum from 0. In particular, in contrast to Eq. (3), the prefactor to the exponential function in Eq. (4) does not depend on \mathbf{u} . We also postulate that for f and f_L^+ there exists a

threshold value of the porosity, φ^* , such that

$$\begin{aligned} u_0 = 0 & \quad \text{for } \varphi_c \leq \varphi < \varphi^*, \\ \gamma = 2 & \quad \text{for } \varphi^* \leq \varphi < 1, \end{aligned} \quad (5)$$

which reduces, by 1, the number of unknown parameters in Eq. (4) for any given φ . This number can be reduced to 2 by noticing that each vdf is normalized to 1. Actually, for $\varphi < \varphi^*$ (which implies $u_0 = 0$) the normalizing constant is given by $a = \gamma/[u_s \Gamma(1/\gamma)]$, where Γ is the gamma function, whereas for $\varphi > \varphi^*$ the vdf is a truncated normal distribution and $a^{-1} = \frac{1}{2} \sqrt{\pi} u_s \operatorname{erfc}(-u_0/u_s)$, where $\operatorname{erfc}(x)$ is the complementary error function. The aim of our paper is to justify Eqs. (4) and (5).

II. THE MODEL

To verify Eq. (4), we examined numerically an effectively two-dimensional model of fibrous materials with the porous matrix built of identical, freely overlapping objects randomly deposited on a regular lattice of size L [19]. We considered two obstacle shapes, disks and squares, both with the hydraulic diameter $a = 8$ lattice units (l.u.). The fluid was assumed to be incompressible and Newtonian, driven by a bulk force (gravity) small enough to ensure the creeping flow ($\operatorname{Re} \ll 1$).

The basic numerical method used to solve the problem was the Palabos [20] implementation of the lattice Boltzmann method (LBM) with the Bhatnagar-Gross-Krook

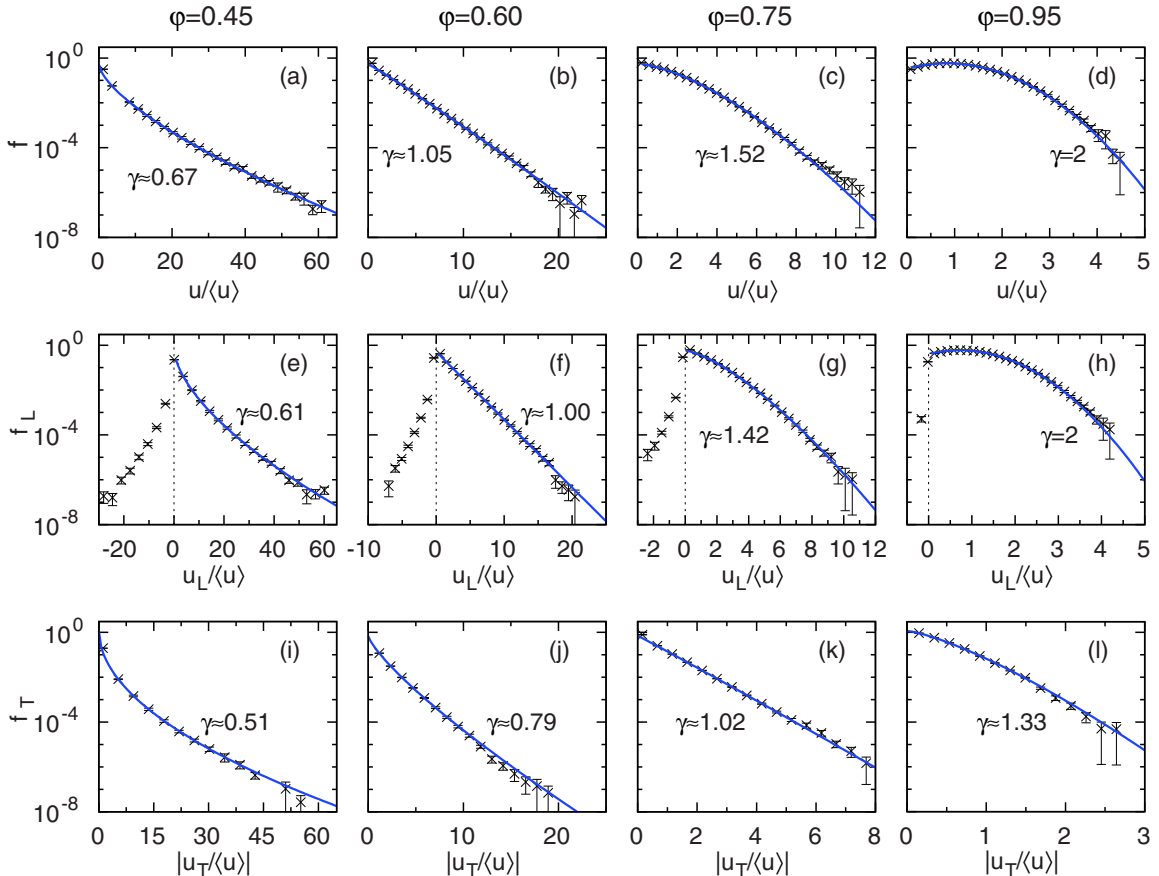


FIG. 1. The velocity distribution function f [panels (a)–(d)], f_L (e)–(h), and f_T (i)–(l) for selected porosities $\varphi = 0.45$ (a), (e), (i), 0.60 (b), (f), (j), 0.75 (c), (g), (k), and 0.95 (d), (h), (l) obtained for overlapping disks. Solid lines show fits to Eq. (4).

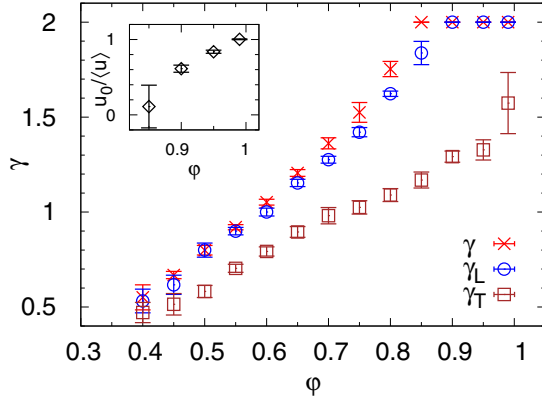


FIG. 2. Exponent γ for f (\times), f_L^+ (\circ), and f_T (\square) as a function of porosity for overlapping disks. Inset: $u_0/\langle u \rangle$ as a function of porosity for f and $\varphi > \varphi^* \approx 0.85$.

approximation for collisions and the numerical viscosity $\nu = 1/6$ [21–23]. While the LBM is often used for solving flows in porous media, its accuracy decreases when the channels in the porous matrix are too narrow. To verify whether this effect is significant in the model of overlapping objects, we also solved it with the finite difference (FD) method. In this case we used only square obstacles arranged so that the minimum channel width was 4 l.u. [21]. In both cases we used the periodic boundary conditions along the macroscopic fluid flow direction. As for the transverse direction, we applied the no-slip boundary conditions in the LBM and periodic ones for the FD. To minimize the finite-size effects, the lattice size, $L = 1000$ l.u. (LBM) and 2000 l.u. (FD) was chosen to ensure that $L/a > 100$ [24] and $2L/a > 25/\sqrt{1-\varphi}$ [25], and the results were compared with those obtained for the system of size $L/2$. The simulation results were averaged over 20 independent porous samples for porosities $\varphi = 0.99, 0.95, 0.9, \dots$ down to the proximity of the percolation threshold $\varphi_c \approx 0.4868$ for the squares [26] and ≈ 0.40 for the disks. The fluid velocity was measured at the underlying lattice nodes and binned to create histograms. In addition, to verify whether our main conclusions depend on the space dimensionality, we performed LBM simulations for the system of overlapping cubes randomly distributed in a 3D space, using $a = 8$ l.u. and $L = 128$ l.u. ($L/a = 16$).

III. RESULTS

Representative results obtained for overlapping disks using the LBM are shown in Fig. 1. All velocities in this figure are normalized by $\langle u \rangle$, and hence effectively dimensionless. All data for f , f_L^+ , f_T , including those not shown, can be fitted well to Eq. (4) constrained by Eq. (5). As the porosity is increased from φ_c toward 1 (which corresponds to the obstacle concentration going to zero), a semilog plot of f changes its shape from convex (subexponential), through linear (exponential), concave (superexponential), parabolic (Gaussian centered at 0), and shifted parabolic (Gaussian shifted toward u). The form of f_L^+ closely follows that of f , but f_L^- vanishes faster than f_L^+ , especially far from φ_c . The exponent γ corresponding to f_T also turns out to be φ -dependent, though its value never reaches 2 (Fig. 2). This

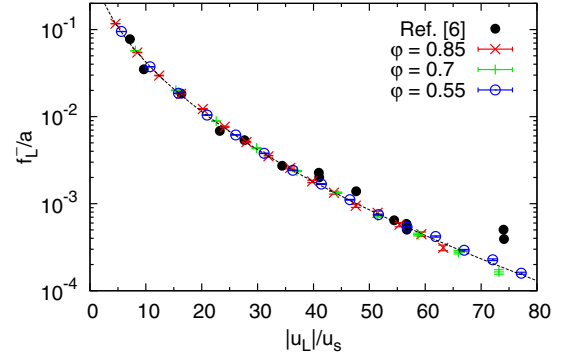


FIG. 3. Scaling of f_L^- according to Eq. (4) with $u_0 = 0$ and γ fixed at 0.5. Open symbols show the results for overlapping squares at porosity $\varphi = 0.55, 0.7, 0.85$; filled circles represent the experimental data of Ref. [6]. The dashed line is the scaling function $g(x) = \exp(-\sqrt{x})$.

extends the experimental findings of Ref. [6], where $\gamma \approx 1$ was reported for f_T at a fixed φ that was chosen far from both φ_c and 1. Note, however, that the current simulations cannot be used to reliably estimate γ for f_T in the limit of $\varphi \rightarrow 1$, as in this limit the number of obstacles becomes very small and hence a large value of L is required to avoid finite-size effects. It is thus possible that in this limit γ tends to 2. The threshold value $\varphi^* \approx 0.85$ for f is close to its counterpart ≈ 0.87 for f_L^+ ; the accuracy of our simulations was insufficient to tell if they are actually different from each other.

As expected, u_0 turns out to be a continuous function of φ , growing from 0 for $\varphi \leq \varphi^*$ to $\langle u \rangle$ for $\varphi = 1$ (Fig. 2, inset). Similar results were obtained for overlapping squares (data not shown).

As for f_L^- , which controls the probability distribution of negative values of u_L , we found that its tail is well described by power-exponential distribution with $\gamma = 0.5$ for all φ (Fig. 3). This conclusion was drawn from simulations for $\varphi \leq 0.85$, as for higher porosities the decay of f_L^- is so rapid, cf. Fig. 1, that no reliable fitting of the data is possible. The value of $\gamma = 0.5$ is also consistent with the experimental results obtained recently in Ref. [6] (Fig. 3) and our simulation data

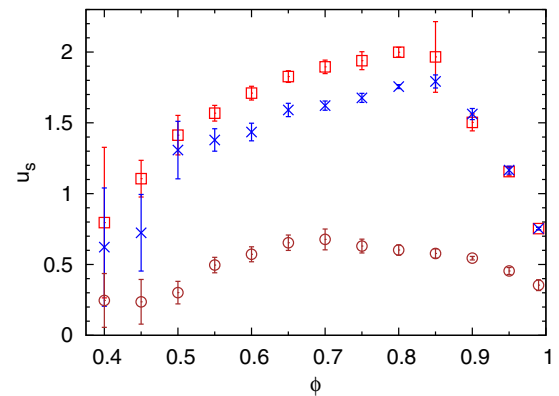


FIG. 4. The scale factor (u_s) as a function of the porosity (φ) for the model of overlapping discs and three vdfs: f (\square), f_L^+ (\times), and f_T (\circ).

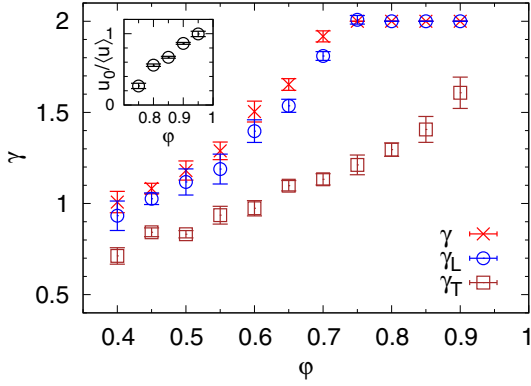


FIG. 5. Exponent γ for f (\times), f_L^+ (\circ), and f_T (\square) as a function of porosity for overlapping cubes. Inset: $u_0/\langle u \rangle$ as a function of porosity for f and $\varphi > \varphi^*$.

for overlapping disks (data not shown). The contribution of f_L^- to the transport is negligible compared to that of f_L^+ only for relatively high porosities. Consequently, simplified theories that assume $f_L^- \equiv 0$ [27] are invalid close to φ_c .

The dependence of the scale factor (u_s) on the porosity is shown in Fig. 4. In the model considered here this dependence is rather weak, although a clear maximum of $u_s(\varphi)$ appears at φ^* . As φ goes to 1, the values of u_s for f and f_L^+ converge, which reflects the fact that in this limit the transverse velocity u_T gets negligible compared to the longitudinal one ($f \approx f_L^+$). As the porosity is lowered, the contribution of u_T to u becomes more and more significant and the scale factor for f becomes larger than for f_L^+ .

Finally, Fig. 5 shows the values of $\gamma(\varphi)$ determined for f , f_L , and f_T in the 3D model of overlapping cubes. Qualitatively, these results are very similar to those shown in Fig. 2 for 2D. One difference is a much lower value of the percolation threshold, $\varphi_c \approx 0.065$ [26]. Another difference is that the value of φ^* is very close to the percolation threshold for the obstacles, ≈ 0.75 [26]. In other words, the range of porosities with $\gamma = 2$ coincides with the porosities for which the porous matrix is composed of isolated islands (in 2D the percolation thresholds for obstacles and for the void phase are the same). The results for the scale factor (u_s) are also similar to those obtained for the 2D case, cf. Fig. 4 (data not shown). However, even though the number of the lattice nodes used in the numerical model was twice as large as in 2D, the ratio of L/a was only 16, a value an order of magnitude smaller than that required to reduce the impact of the finite-size effects on the permeability tensor below 5% [28]. It is also known that the permeability of a finite sample of size L smaller than the representative elementary volume (REV) is an increasing function of L [28], which suggests that taking too small system sizes may influence the tails of the velocity distributions. This may explain our observation that the fits of our data to Eq. (4) are unsatisfactory for very diluted ($\varphi \gtrsim 0.95$) and dense systems ($\varphi \lesssim 0.35$).

IV. DISCUSSION AND CONCLUSIONS

Our findings lead to the following general picture of the fluid velocity distributions at $u \gtrsim \langle u \rangle$. At the percolation threshold all four velocity distribution functions, f , f_L^+ , f_L^- ,

and f_T decay in accordance with the power-exponential distribution Eq. (4) with $u_0 = 0$ and $\gamma = 1/2$. As the porosity is increased, γ remains constant for f_L^- , but increases for f , f_L^+ , and f_T . At some threshold porosity φ^* the exponent γ determined for f or f_L^+ reaches the maximum value of 2. As the porosity is increased above φ^* , γ stays fixed at 2, whereas parameter u_0 becomes φ -dependent and grows from 0 to $\langle u \rangle$ as φ approaches 1. Therefore, a vdf in a random porous medium is either subexponential ($\gamma < 1$), exponential ($\gamma = 1$), superexponential ($2 > \gamma > 1$), or normal ($\gamma = 2$). If $\gamma = 2$, the corresponding vdf depends on the porosity through the shift parameter u_0 .

The significance of Eq. (4) is related to several factors. First, it describes the statistical properties of the microscopic velocity field for the velocities $u \gtrsim \langle u \rangle$ that have a major contribution to the advective transport. Unlike the case of inviscid fluid, a *viscous* fluid flowing in a *random* porous medium, no matter how rarified, forms a highly nonuniform velocity field that is very sensitive to the distribution of the obstacles [24], and Eq. (4) ensures that there is some order in this complexity. Second, it is a relatively simple formula with only two unknown parameters at any given porosity. Third, the dependence of at least one of these parameters, γ , on the porosity also appears to be fairly simple: in the model studied here it could be roughly approximated with two straight line segments (Fig. 2). Given this simplicity, Eq. (4) might be used to link porosity with vdf-dependent macroscopic parameters like permeability or tortuosity. It should also be useful in studies on several open issues, like the microscopic foundations of permeability and hydrodynamic dispersion (longitudinal and transverse) of passive solutes [29–31], the physical relevance of the tortuosity [32], and properties of the conducting backbone [30], all with immediate practical applications.

Equation (4) is a phenomenological one and we are not aware of any theoretical work explaining its form even in the limit of the diluted system, $\varphi \rightarrow 1$. Actually, this limit was investigated in the context of hydrodynamic dispersion using an effective medium approximation, and the correction to the solution of the flow past a single sphere due to interactions with other spheres was found [33,34], but that solution does not predict any interesting phenomena for the velocities larger than the bulk velocity $\approx \langle u \rangle$. We believe that the correct theoretical approach to this problem must focus on the flow channelization resulting from the local fluctuations in the obstacle distribution. While an attempt toward a theory of this kind was recently proposed in Ref. [8], it is based on too many *ad hoc* assumptions to be regarded as satisfactory.

Some important questions remain open. For example, to what extent our hypothesis remains valid for porous matrices with a complex, highly correlated structure [35]. Another problem is whether the value of $\gamma = 2$ for f and f_L^+ actually implies the absence of long-range correlations in the velocity field above φ^* [6] or perhaps these correlations do remain and require that the power-exponential distribution be supplemented with some less significant terms. The physical nature of φ^* also remains unclear.

In summary, we propose that a general form of the velocity distribution functions in disordered porous media is given by

a power-exponential distribution with the shape factor γ and location parameter u_0 such that $1/2 \leq \gamma \leq 2$ and either $u_0 = 0$ or $\gamma = 2$. Moreover, γ has a universal, porosity-independent

value $1/2$ both at the percolation threshold and for the negative part of the velocity component parallel to the macroscopic fluid-flow direction.

-
- [1] C. L. N. Oliveira, J. S. Andrade, and H. J. Herrmann, *Phys. Rev. E* **83**, 066307 (2011).
- [2] X. Li, J. Huang, and A. Faghri, *Energy* **81**, 489 (2015).
- [3] R. Penta and D. Ambrosi, *J. Theor. Biol.* **364**, 80 (2015).
- [4] Y. E. Kutsovsky, L. E. Scriven, H. T. Davis, and B. E. Hammer, *Phys. Fluids* **8**, 863 (1996).
- [5] P. Mansfield and B. Issa, *J. Magn. Reson. Ser. A* **122**, 137 (1996).
- [6] S. S. Datta, H. Chiang, T. S. Ramakrishnan, and D. A. Weitz, *Phys. Rev. Lett.* **111**, 064501 (2013).
- [7] M. Morad and A. Khalili, *Exp. Fluids* **46**, 323 (2009).
- [8] M. Holzner, V. L. Morales, M. Willmann, and M. Dentz, *Phys. Rev. E* **92**, 013015 (2015).
- [9] J. S. Andrade, M. P. Almeida, J. Mendes Filho, S. Havlin, B. Suki, and H. E. Stanley, *Phys. Rev. Lett.* **79**, 3901 (1997).
- [10] J. S. Andrade, U. M. S. Costa, M. P. Almeida, H. A. Makse, and H. E. Stanley, *Phys. Rev. Lett.* **82**, 5249 (1999).
- [11] A. Duda, Z. Koza, and M. Matyka, *Phys. Rev. E* **84**, 036319 (2011).
- [12] J. Bear, *Dynamics of Fluids in Porous Media* (Elsevier, New York, 1972).
- [13] B. Bijeljic, A. Raeini, P. Mostaghimi, and M. J. Blunt, *Phys. Rev. E* **87**, 013011 (2013).
- [14] A. D. Araújo, W. B. Bastos, J. S. Andrade, Jr., and H. J. Herrmann, *Phys. Rev. E* **74**, 010401(R) (2006).
- [15] L. Lebon, L. Oger, J. Leblond, J. P. Hulin, N. S. Martys, and L. M. Schwartz, *Phys. Fluids* **8**, 293 (1996).
- [16] R. S. Maier, D. M. Kroll, H. Davis, and R. S. Bernard, *J. Colloid Interf. Sci.* **217**, 341 (1999).
- [17] R. S. Maier, D. M. Kroll, Y. E. Kutsovsky, H. T. Davis, and R. S. Bernard, *Phys. Fluids* **10**, 60 (1998).
- [18] M. Siena, M. Riva, J. D. Hyman, C. L. Winter, and A. Guadagnini, *Phys. Rev. E* **89**, 013018 (2014).
- [19] M. M. Tomadakis and S. V. Sotirchos, *J. Chem. Phys.* **98**, 616 (1993).
- [20] www.palabos.org.
- [21] S. Succi, *The Lattice Boltzmann Equation for Fluid Dynamics and Beyond* (Clarendon Press, New York, 2001).
- [22] C. Huber, A. Parmigiani, J. Latt, and J. Dufek, *Water Resour. Res.* **49**, 6371 (2013).
- [23] C. Pan, L.-S. Luo, and C. T. Miller, *Comput. Fluids* **35**, 898 (2006).
- [24] Z. Koza, M. Matyka, and A. Khalili, *Phys. Rev. E* **79**, 066306 (2009).
- [25] A. Hendrick, R. Erdmann, and M. Goodman, *Transp. Porous Media* **95**, 389 (2012).
- [26] Z. Koza, G. Kondrat, and K. Suszczyński, *J. Stat. Mech.* (2014) P11005.
- [27] C. Fleurant and J. van der Lee, *Math. Geol.* **33**, 449 (2001).
- [28] M. Matyka, Z. Koza, J. Gołembiewski, M. Kostur, and M. Januszewski, *Phys. Rev. E* **88**, 023018 (2013).
- [29] M. Sahimi, *Rev. Mod. Phys.* **65**, 1393 (1993).
- [30] A. Hunt, *Percolation Theory for Flow in Porous Media*, Lecture Notes in Physics (Springer, Berlin, 2009).
- [31] M. Icardi, G. Boccardo, D. L. Marchisio, T. Tosco, and R. Sethi, *Phys. Rev. E* **90**, 013032 (2014).
- [32] B. Ghanbarian, A. G. Hunt, R. P. Ewing, and M. Sahimi, *Soil Sci. Soc. Am. J.* **77**, 1461 (2013).
- [33] D. L. Koch and J. F. Brady, *J. Fluid Mech.* **154**, 399 (1985).
- [34] A. Acrivos, E. J. Hinch, and D. J. Jeffrey, *J. Fluid Mech.* **101**, 403 (1980).
- [35] L. Rong, K. Dong, and A. Yu, *Chem. Eng. Sci.* **99**, 44 (2013).